Article ID 1004-924X(2004)04-0386-07

Electro-optic modulators with self-assembled superlattice waveguides

SUN De-gui[1], LIU Zhi-fu[1], HO Seng-tiong[1], KANG Hu[2], ZHU Pei-wang[2], MARKS Tobin[2]

(1. *Department of Electrical and Computer Engineering, Northwestern University, Evanston, IL 60208, USA*;
2. *Department of Chemistry and Materials Research Center, Northwestern University, Evanston, IL 60208, USA*)

Abstract: This paper reports a new waveguide electro-optic (EO) modulator with self-assembled superlattice (SAS) electro-optic films. This work focuses on the measurement for the EO coefficient of SAS films and the optimization for the devices structure. In order to have a precise and effective design, we test the angle-dependence of the second harmonic generation of incident laser beam to determine the effective EO coefficient. We study he absorptive loss of electrodes of devices with the optical propagation theory of multi-layered films and optimize the devices structure to obtain the lowest drive voltage. The paper gives the structure of experimental samples and the scanned electronic microscopy (SEM) pictures of our fabricated devices. Finally, 1.0 dB/cm optical propagation loss of the EO modulators is achieved, which agrees with the experimental results.

Key words: electrooptic modulator; self-assembled superlattice; waveguide; optical propagation loss; propagation matrix

自聚焦超晶格波导电光调制器

孙德贵[1], 刘志福[1], HO Seng-Tiong[1], 康 虎[2], 朱培旺[2], MARKS Tobin[2]

(1.美国西北大学 量子光学实验室, 埃维斯顿 伊利诺斯州 60208;
2.美国西北大学 化学系, 埃维斯顿 伊利诺斯州 60208)

摘要: 研制了一种基于自聚焦超晶格薄膜电光波导调制器。首先给出了自聚焦超晶格薄膜电光特性的测量和器件结构的优化设计, 采用测量二次谐波生成值对入射角的依赖关系测定了薄膜的有效电光系数, 保证了器件的设计精确有效。利用多层膜传输理论研究了器件电极对光波的最大吸收, 并对器件结构进行了优化, 获得了最小调制电压。其次给出了所加工的实验模型结构和扫描电子显微镜(SEM)图片, 确保了加工质量和设计结果的一致。研究结果表明: 这种无需外电场极化处理的新型聚合物薄膜电光调制器加工难度小, 并且光学损耗优化到了1.0 dB/cm。

关 键 词: 电光调制器; 自聚焦超晶格; 波导; 光传输损耗; 传输矩阵
中图分类号: TN252 文献标识码: A

Received date: 2004-03-24; **Revised date:** 2004-06-05.
Foundation item: This work supported by DARPA/ARO, and the MRSEC Program of NSF at Northwestern University.

1 Introduction

An electro-optic (EO) modulator is the central component in the modern optical communication. Its main performance is evaluated in terms of the so-called modulating bandwidth, which depends on both the EO cofficient of materials and the structure of devices. Organic materials containing molecular units with large second-order nonlinear susceptibilities are attractive for high speed lightwave modulation[1-5]. In particular, polymer-based electro-optic (EO) modulators have been studied for a few decades and had impressive accomplishments in research such as the demonstration for high-speed modulation from 40 GHz to 110 GHz[3-5]. Polymers, as new kinds of EO materials in high-speed devices, have essential advantages over conventional ferroelectric materials such as $LiNbO_3$ in the EO properties of the material, the ease in fabrication of devices, and the convenience in geometrical design and performance optimization of devices. Polymers have similar microwave dielectric and light wave dielectric constants, which enable high-speed EO modulators with significant potential in optimization. Polymer-based devices are easy to be fabricated with micro-strip electrode geometries that give a large optical/electrical overlap in modulation of devices[4-5]. However, polymers, especially the poled polymers, still present critical challenges before polymer-based EO devices are commercialized. These challenges include an undesirable intrinsic optical absorption, poling-induced damage to the physical properties, and a lack of substantiated proof of long-term stability. The self-assembled superlattice (SAS) classes of materials[6-8] have potentially larger nonlinear EO responses than conventional glassy polymers and do not require electric field poling. Thus, they are attractive for high-speed, low drive-voltage EO modulating devices and have temporal stability of the EO properties[9]. The SAS-based EO modulator requires different considerations in device optimization from those of poled-polymer EO modulator structures. This paper reports an optimized structure to achieve low modulation voltages in SAS-based modulators with minimum absorption loss while maintaining high modulation speed.

2 Calculation and analysis for optical loss

The SAS samples have been characterized by a variety physicochemical techniques, including optical spectroscopy, aqueous contact-angle measurement, specular X-ray reflectivity, atomic force microscopy, and angle-dependent polarized second harmonic generation as shown in Fig. 1, and then the EO coefficient with a referenced material having the known EO coefficient. The current challenge for using SAS materials in waveguiding EO modulators is the SAS thickness in order to have an efficient electrical/optical overlap in the SAS film. Recently, the reliable SAS thickness that can be achieved was increased to 0.2~0.4 μm. However, this thickness is insufficient for the SAS component to be the sole core layer of an EO modulator waveguide. Thus, the polymer benzocyclobutene (BCB), which has a refractive index close to that of the SAS film, is introduced with the SAS film in the device structure. Figure 2 shows a schematic of a modulator using the SAS material as the EO-active component. Here the upper cladding layer is

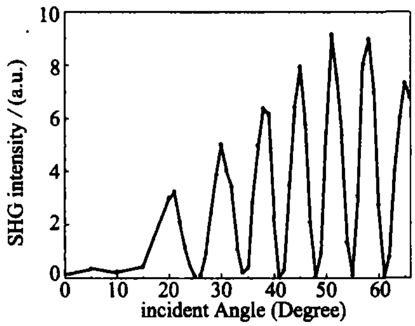

Fig. 1 SHG response as a function of fundamental beam incident angle from a float glass slide having an SAS bilayer on either side

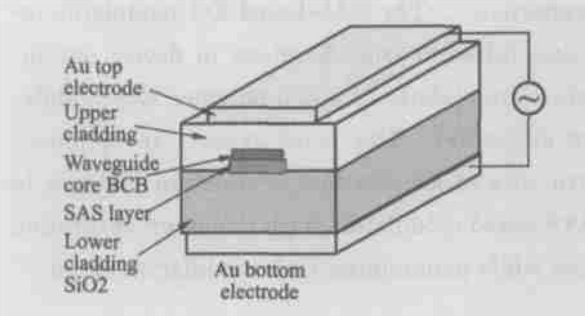

Fig.2 Schematic of an SAS-based EO modulator

the polymer CYTOP, the lower cladding layer is SiO_2, and the electrode is gold[10-11]. An EO waveguide phase modulator is firstly required to have a relatively low half-wave drive-voltage defined by,

$$V_\pi = \frac{\lambda D}{n^3 r \Gamma \cdot L} , \quad (1)$$

where λ is the wavelength of light wave in free space, r the EO coefficient of the SAS film, n the optical refractive index of the SAS film, D the distance between the upper and lower electrodes, and Γ the overlap integral of optical and electrical fields in the waveguide.

3 Theoretical study

In order to achieve a low half-wave drive voltage, it is desirable to minimize the distance between the top and the bottom Au electrodes by minimizing the upper and lower cladding thickness. However, when the cladding thickness is small, the optical modes will begin to have substantial optical loss, especially for the TM modes, due to optical absorption by the Au electrodes. Another impact of changing the electrode distance is the change in the propagation impedance of the parallel plate transmission lines formed by the top and bottom electrodes referred to as micro-strip electrodes. Namely, a low optical loss design is crucial for an SAS-based EO modulator when the thickness of SAS film is insufficient as a sole core of the modulator waveguide. So to achieve this goal, a fast and efficient theoretical method has been demonstrated[10]. This method offers a numerical analysis of vertical wave propagation in waveguides with arbitrary refractive properties for calculating the modal properties in a waveguide with an arbitrary refractive index distribution. This method efficiently approximates a planar waveguide cross-section by a finite number of thin dielectric layers into a 2×2 transfer matrix to relate adjacent layers. If the waveguide system contains N layers labeled by 1, 2, . . . , N, and the layer 0 is the substrate, the angle for the lowest-order guided mode corresponds to the lowest angle that results in a local maximum for the field excitation in the waveguide, which is referred to as the fundamental mode, and hence a local maximum transmittance is formed in the waveguide. This angle can be used to propagate through the medium and calculate the field at each layer in the waveguide as a function of space. At the interface between layer i and layer $i+1$, the corresponding indices are n_i and n_{i+1}, and the corresponding angles are θ_i and θ_{i+1}, the formula for calculating θ_{i+1} is given by $\theta_{i+1} = \arcsin[(n_i \sin\theta_i)/n_{i+1}]$. The TE propagation vectors on each side of the interface are then $g = (2\pi n_i \cos\theta_i)/\lambda$ and $h = (2\pi n_{i+1}\cos\theta_{i+1})/\lambda$. The TM propagation vectors are $g = (2\pi\cos\theta_i)/\lambda n_i$ and $h = (2\pi\cos\theta_{i+1})/\lambda n_{i+1}$. The transmission and reflection coefficients at the interface are $T = 2g/(g+h)$ and $R = (g-h)/(g+h)$ for the left-hand side of the interface and $T_p = 2h/(g+h)$ and $R_p = (g-h)/(g+h)$ for the right-hand side of the interface. If E_1^+ and E_1^- are the electric fields of the forward and backward beams in the input side, respectively, and E_N^+ and E_N^- are the electric fields of the forward and backward beams in the output side, respectively, the relation between the output side and the input side of the system can be defined by[9-10]

$$\begin{pmatrix} E_N^+ \\ E_N^- \end{pmatrix} = \left(\prod_{i=1}^{N-1} A_i\right) \cdot \begin{pmatrix} E_1^+ \\ E_1^- \end{pmatrix} , \quad (2)$$

where A_i is defined by

$$A_i = \begin{pmatrix} \exp(jhd) & 0 \\ 0 & exp(-jhd) \end{pmatrix} \times \begin{pmatrix} TT_p - RR_p & \frac{R_p}{T_p} \\ -\frac{R}{R_p} & \frac{1}{T_p} \end{pmatrix}, \quad (3)$$

For any detailed discussion on the numerical method and the use of relevant transfer matrix, please see Refs. 10 and 11.

4 Optimization for optical loss

In this work, we are mainly concerned with the optical absorption loss of Au, so we only simulate the TM mode. In the simulation, the wavelength in free space is $\lambda = 1\ 550$ nm. At this wavelength, we take the refractive index of the core layer material BCB as $n_b = 1.54$, which is very close to the measured value of refractive index of the SAS film, the refractive index of the lower cladding layer SiO_2 $n_s = 1.45$, and the refractive index of the upper commercially available cladding layer CYTOP $n_c = 1.34$[12-13]. In addition, the Au, as the electrode material, has a complex index expressed as $n = 0.38 + 10.4i$. We know that the thickness of the core layer, and of the upper and the lower cladding layers directly impacts the Au electrode absorption loss, and both the upper and the lower Au electrodes have the same level of absorption losses. In order to have same easily testable samples, we omitted the upper Au electrode by using a sufficiently thick CYTOP upper cladding layer. In accordance with the experimental results, when the thickness of the upper cladding layer CYTOP is 1.0 μm, the absorption loss induced by the upper Au electrode can be ignored. Accordingly, we mainly studied the influences of the waveguide core layer BCB thickness and the thickness of the lower cladding layer, SiO_2. First, two typical results are the relationship between the Au absorption loss and BCB thickness as shown in Fig. 3(a), and the relationship between the Au absorption loss and SiO_2 thickness as

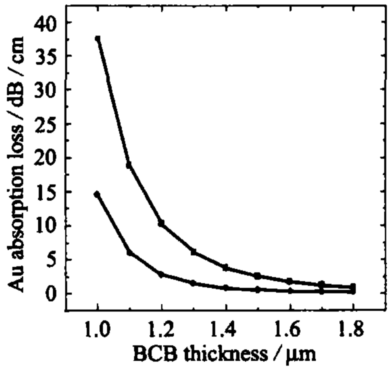

Fig. 3(a) Au absorption vs. BCB thickness for different SiO_2 cladding thicknesses: solid squares are for 2.0 μm SiO_2 and solid circles are for 2.5 μm SiO_2

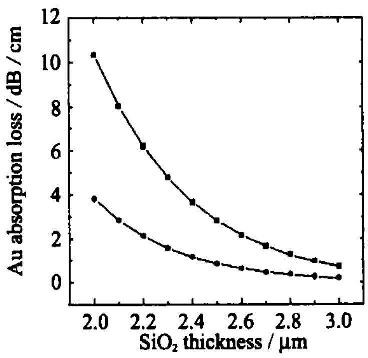

Fig. 3(b) Au absorption vs. SiO_2 thickness for different BCB thickness: solid squares are for 1.2 μm BCB and solid circles are for 1.4 μm BCB

shown in Fig. 3(b). Note from Fig. 3(a) that the thickness of both the lower cladding layer SiO_2 and the waveguide core layer impacts the optical absorption loss of the bottom Au electrode. At both the 2.0 μm and 2.5 μm thickness of SiO_2, the optical absorption loss of the Au film quickly decreases with the thickness of the waveguide core layer BCB in the range from 1.1~ 1.4 μm, but it slowly decreases when the BCB thickness is larger than 1.4 μm. Our simulation shows that the thickness range of the waveguide core BCB layer for single-mode operations at 1 550 nm wavelength is 1.0~ 1.4 μm. Note from Fig. 3(b) that when the SiO_2 thickness is larger than 2.6 μm and the BCB thickness is 1.4 μm, the Au absorption is less than 1.0

dB/cm. For the EO waveguide modulator, the Au absorption loss of less than 1.0 dB/cm is sufficient for achieving a low half-wave drive voltage Vπ and very helpful for increasing the device length in fabrication of SAS based EO modulators. The absorption loss induced by the top electrode can be simulated with an inverse construction as that in the case of bottom electrode, and the sum of these two cases is total absorption loss of the system. In accordance with the simulated results as shown in Fig. 3(a) and Fig. 3(b), we fabricated some devices having different thickness values of SiO_2: 2.0 μm and 2.65 μm, and two different thickness values of BCB layers: 1.2 μm and 1.4 μm. These samples are used for analyzing the waveguide quality and the propagation loss measurements. A typical SEM perspective image of the waveguide before the upper cladding CYTOP was coated is shown in Fig. 4(a), and a typical SEM cross-sectional image of device after the upper cladding was coated is shown in Fig. 4(b). The experimental results are summarized in Table I. In the experiments, the coupling loss at the two ends of the test device could be estimated. Note that the experimental results agree well with the simulated values.

Tab. 1 Experimental results of optical loss induced by the bottom electrode (λ= 1 550 nm)

SiO_2 Thickness (μm)	Core BCB Thickness (μm)	Metal Loss (dB/cm)
2.00	1.0-1.1	~ 20
2.65	1.1-1.2	~ 7.0
2.65	1.3-1.4	< 1.0

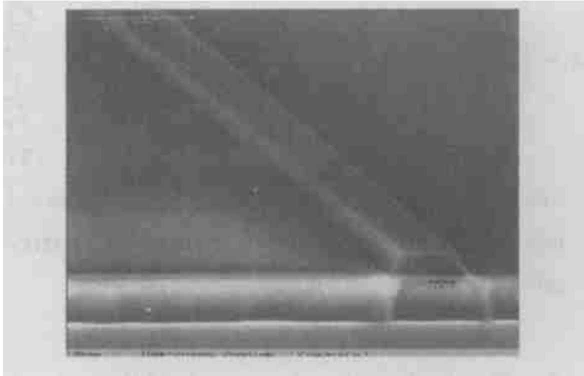

Fig. 4(a) SEM perspective image of BCB and SAS-based waveguide channel before upper cladding layer CYTOP deposition for EO modulator.

Fig. 4(b) SEM cross-sectional image of an SAS-based EO modulator

5 Discussion

The present simulation and experimental results provide important guidance not only for fabrication of SAS-based EO modulators with BCB co-guiding layers, but also for the modulators having SAS materials as the exclusive guiding layer. With the efficient loss-minimizing design of devices, the reliable physical properties, and steadily increasing thicknesses obtained for SAS films, relatively high EO coefficients of more than 15 pm/V, and progressively decreased half-wave drive voltages have been achieved with 1.5 cm long devices[14-15]. In the future, with further improvements in SAS physical properties and increased of thickness of SAS films, combined with the performance optimization of devices discussed here to maximize the electrical/optical overlap factor, half-wave drive voltages will be continuously decreased to less than 1~5 V. The above studies on minimizing optical propagation loss are for the case in which the thickness of SAS film is not sufficient and a filling waveguide material (in this case BCB) is used to compensate the waveguide core layer. Thus, the optical constants in the present simulation are from the filling material. With the improvement of SAS film growth techniques, the thickness of SAS film will be progressively increased without loss of EO properties.

As mentioned above, another main factor impacting the half-wave drive voltage V_π is the electrical/optical overlap integral Γ. For the EO modulator shown in Fig. 2, the SAS film is placed at the bottom of the core layer of waveguide, which is the most convenient way of placing the SAS film. In fact, it can be put at any height within the core layer of waveguide in order to obtain a maximum electrical/optical overlap integral.

6 Conclusions

In summary, as a new kind of electrooptic material, the SAS films discussed here have high EO coefficients without external field poling, so they offer many advantages over poled polymers. In fact, this feature is especially attractive for modulating devices. Previously, the thickness of SAS films has not been sufficient as a sole waveguide core layer, so it has been necessary to implement the loss-minimizing design reported here in multiplayer structures, and a desirable half-wave drive voltage has been achieved. However, even when the thickness of SAS films is sufficient for a waveguide core layer, the loss minimizing designs presented will still be advantageous. The present research shows that the two main optical constants of the SAS films, the refractive index and the absorption coefficient at the wavelength of 1 550 nm, are somewhat higher than that of BCB co-guiding layer. In this work, excellent agreement between experimental and the simulated results of optical loss have been achieved. In addition, the impact of the optimization of the electrical/optical overlap integral has been analyzed in terms of the location and thickness of the SAS film. Therefore, this work is not only a necessary step to achieve low loss in the SAS-based EO modulators, but it also gives us confidence achieving half-wave drive voltage below 1~5 V when the thickness of the SAS film is sufficient to be the sole waveguide core layer. Second-generation SAS materials with far higher r coefficients should improve these parameters even better.

This work was supported by DARPA/ARO, and the MRSEC program of NSF at Northwestern University.

参考文献:

[1] SHUTO Y, TOMARU S, HIKITA M, *et al*. Optical intensity modulators using diazo-dye-substituted polymer channel waveguides[J]. *IEEE J. Quantum. Electron*, 1995, 31(8): 1451-1460.

[2] CHEN D, FETTERMAN H R, CHEN A, *et al*. D. Demonstration of 110 GHz electro-optic polymer modulators[J]. *Appl. Phys. Lett.*, 1997, 70(25): 3335-3337.

[3] ELDADA L, SHACKLETTE W. Advances in polymer integrated optics[J]. *IEEE J. Selected Topics Quantum Electron*, 2000, 6(1): 54-68.

[4] OH M C, ZHANG H, ZHANG C, *et al*. Recent advances in electro-optic polymer modulators incorporating highly nonlinear chromophore[J]. *IEEE J. Selected Topics Quantum Electron*, 2001, 7(2): 826-835.

[5] GILL D M, CHOWDHURY A. Electro-optic polymer-based modulator design and performance for 40 Gb/s system applications[J]. *J. Lightwave Technol.*, 20002, 20(12), 2145-2153.

[6] ZHU P, Van der BOOM M E, MILKO E, *et al*. Realization of expeditious layer-by-layer siloxane-based Self-assemly as an efficient route to structurally regular acentric superlattices with large electro-optic responses[J]. *Chem. Mater.*, 2002, 14: 4982-4949.

[7] Van der BOOM M E, ZHU P, EVMENENKO G, *et al*. Nanoscale consecutive self-Assembly of thin-film molecular materials for electrooptic switching. chemical streamlining and ultrahigh response chromophores[J]. *Langmuir*, 2002, 18: 3704-3707.

[8] EVMENENKO G, DUGAN S W, KMETKO J. Specular X-ray reflectivity study of ordering in self-assembled organic-inorganic electro-optic multilayer films[J]. *J. Chem. Phys.*, 2001, 115: 6722-6727.

[9] LIN W B, LIN W P, WONG G K, *et al*. Supramolecular approaches to second-order nonlinear optical materials. Self-assembly and microstructural characterization of intrinsically acentric [(Aminophenyl) azo] pyridinium superlattices[J]. *J. Am. Chem. Soc.*, 1996, 118: 8034-8042.

[10] RAFIZADEH D, HO S T. Numerical analysis of vectorial wave propagation in waveguides with arbitrary refractive index profiles[J]. *Optics Communications*, 1997, 141: 17-20.

[11] SUN D G, WANG N X, WENG Z H, *et al*. Calculation and design for bistable optical devices of nonlinear interference filters[J]. *Opt. Eng.*, 1993, 32: 63-66.

[12] BCB 3022-25, from Dow Chemical Co., Midland, MI 48674[Z].

[13] Asahi Glass Co., C/O Bellex International Corp., Wilmington, DE 19809[Z].

[14] MARKS T J, HO S T, LIU Z, *et al*. Electro-optic waveguide modulators by the integration of self-assembled superlattices with polymeric and semiconductor materials[J]. *SPIE*, 2003, 4991: 143.

[15] LIU Z, SUN D G, MA J, *et al*. Self-assembled superlattice thin film waveguide electro-optic phase modulators[C]. *CTuS2, CLEO 2003 Conference, Baltimore, MD*, 2003.

作者简介: SUN De-gui: He was born in Jilin Province of China in 1960. He earned his B. S. degree in geometrical optics and optical engineering from Harbin Institute of Technology of China in 1985. He earned his M.S and Ph.D degrees in optical physics, opto-electronic devices and applications from Changchun Institute of Optics and Fine Mechanics, Chinese Academy of Sciences of China in 1988 and 1993, respectively. As a postdoctoral fellow, he ever worked on research on polymeric waveguide electrooptic(EO) modulators and other EO devices in Microelectronics Research Center of the University of Texas at Austin of US from 1994 to 1997. As a technical leader, he ever joined a startup company in Canada from 1998 to 2001 and worked on development of the passive components. As a resarch associate, he was also engaged in research on new high-performance EO modulators in Northwestern University of US from 2002 to 2003. Now he is a professor and Ph.D degree director in Changchun Institute of Optics, Fine Mechanics and Physics, Chinese Academy of Sciences of China. His research interests include integrated optoelectronic components, high-performance EO modulators, new optical networks and related technologies, new optical telecommunications systems and their applications in industry.